CONF-840570--16

[Invited Talk presented at the American Society for Metals Meeting on Materials for Energy Systems, May 1-3, 1984, Washington, DC]

CONF-840570--16

DE85 007543

SURFACE MODIFICATION OF SOLIDS

B. R. Appleton

SOLID STATE DIVISION
OAK RIDGE NATIONAL LABORATORY
Operated by
MARTIN MARIETTA ENERGY SYSTEMS INC.
under contract
DE-AC05-84OR21400
for the
UNITED STATES DEPARTMENT OF ENERGY
Oak Ridge, Tennessee

May 1984

DISCLAIMER

THE USE OF ION BEAM AND PULSED LASER PROCESSING is reviewed for the near-surface modification of a wide range of materials. The techniques of ion implantation doping, ion beam and laser mixing, and pulsed-laser annealing are stressed with particular emphasis on the nonequilibrium aspects of these processing techniques and on new materials properties which can result. Examples are presented illustrating the utility of these techniques for fundamental materials research as well as practical surface modifications.

Ion beam and laser processing techniques have achieved increasing acceptance in recent years both as tools for basic materials research and development and as techniques for modifying the near-surface properties of materials. The success of these techniques in materials research arises because they are nonequilibrium processing methods capable of inducing materials interactions not possible with more conventional equilibrium methods. Consequently, these techniques allow tests of fundamental materials interactions under conditions not heretofore achievable and often result in new materials properties. In addition to these attributes, the inherent control, precision and versatility of these processing techniques have made them particularly suitable for near-surface modification of a variety of materials for technological applications. In this article the characteristics of ion implantation doping, ion beam mixing, and pulsed-laser processing will be reviewed. The nonequilibrium aspects of these techniques and resulting new materials alterations will be stressed. Examples of their use for fundamental materials research and development as well as for practical surface modifications will be presented. For a more comprehensive review of

*Operated by Martin Marietta Energy Systems, Inc. under contract DE-AC05-84OR21400 with USDOE.

the pertinent ion and laser interactions in solids and their applications to materials processing the reader is referred to several recent review sources.[1-17]

ION BEAM AND LASER PROCESSING

ACCELERATOR AND LASER FACILITIES - The experimental apparatus utilized for most of the work discussed here is shown schematically in Fig. 1. The facilities represented in Fig. 1 are part of the Surface Modification and Characterization (SMAC) facilities in the Solid State Division at Oak Ridge National Laboratory. A variety of ion accelerators and lasers are integrated into several common ultrahigh vacuum (UHV) processing and analysis chambers. This arrangement makes it possible to alter the near-surface properties of materials by ion implantation doping, ion beam mixing, and/or pulsed laser annealing in a controlled UHV environment, and to characterize the materials properties in situ by ion beam or surface analysis techniques. A variety of variable temperature/position sample holders can be used for materials processing from 5-1300 K, and goniometers are available which allow for analysis by position ion channeling techniques.

The accelerators include a 2.5-MV Van de Graaff type accelerator used for ion beam analysis; a 200-KV ion implantation accelerator capable of producing high currents of most elements in the periodic table; and a 1.7-MV tandem type accelerator used for both ion beam and nuclear reaction analysis and high energy heavy ion implantation. The available lasers include two Q-switched ruby lasers (0.694 μm wavelength, 15-50 x 10^{-9} s pulse duration, 3 joules total energy) and an excimer laser (0.249 μm, 25 x 10^{-9} s, 1 joule).

ION IMPLANTATION DOPING - Ion implantation doping is a precise, controllable, reproducible and selective method for introducing impurities into solids. Virtually any species of ion can be produced in the versatile ion sources

Fig. 1 - Schematic representation of the ORNL ion beam and laser processing facilities.

available on commercial ion implanters. Mass and energy analysis of the ions before ion implantation insures extreme purity, even isotopic selection of dopants. The implanted concentration is precisely determined from current integration. The depth distribution of the implanted impurity can be precisely controlled by varying the ion energy, and the spatial distribution is controlled by scanning and/or focussing the beam.

Calculated range and damage distributions for 1×10^{16} As atoms/cm^2 implanted into Si at 100 keV are represented in Fig. 2. The implanted As profile ends up as a Gaussian distribution around a projected range of 0.057 μm with a peak concentration of ~3 at.%. Implantation profiles can be "tailored" by varying the energy (depth) and dose (concentration) as desired. As a consequence of the implantation process the incident As ions deposit a substantial fraction of their energy into nuclear collisions which displace Si atoms from their normal lattice sites. This so-called damage energy distribution is shown as the dashed curve in Fig. 2 of nuclear stopping, S_n, versus depth. It can be shown from radiation damage calculations for this case[17] that near the peak of the damage distribution (S_n ~ 1.0 MeV/μm, 0.02 μm) each Si atom is displaced about 55 times. The radiation damage and the details of the collision cascade for each individual ion are important factors in determining the final materials properties during ion implantation. These factors are discussed more in the next subsection.

The materials properties which result from ion implantation doping are governed by many diverse factors. For many materials small amounts of the appropriate implanted dopant can alter or even dominate the electrical, chemical, mechanical or optical properties. These effects can arise from alterations

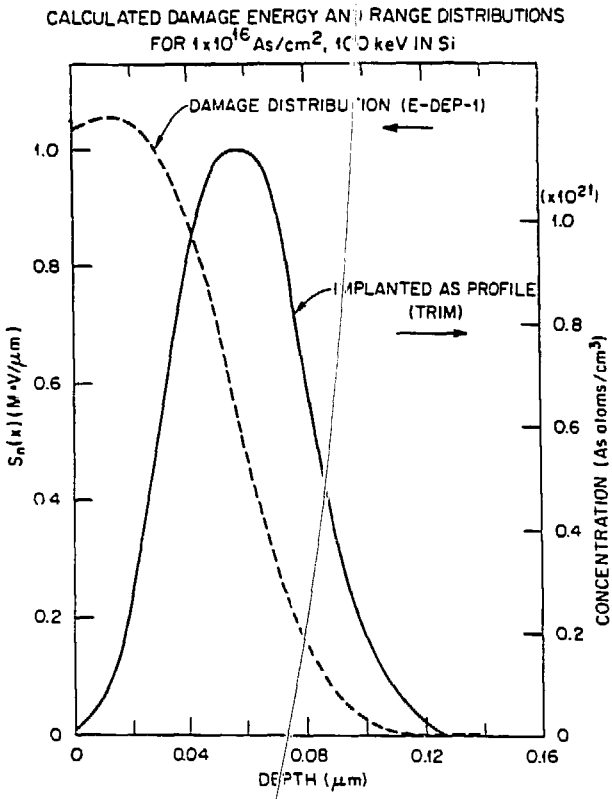

Fig. 2 - Calculated damage energy, S_n, and concentration versus depth profiles for As implanted in Si.

of the local chemistry or metallurgy of the solid; from alterations of the surface microstructure due to radiation damage or induced stress or strain; or from the formation of a new metastable surface alloy induced by several factors working in concert.

The nonequilibrium aspects of ion implantation doping arise because this method of introducing impurities into solids can circumvent many of the constraints which limit equilibrium processing methods. Limitations due to diffusion rates and solid solubility limits can usually be avoided, thermodynamic constraints on phase structure can be relaxed after the collision cascade event, and the implantation process can induce and stabilize metastable phase formation. Specific examples of these various occurences can be found in the references listed.[1-17]

ION BEAM MIXING - As the schematic in Fig. 3 implies, if a thin film of one material B is deposited on a substrate material A and bombarded with energetic heavy ions, materials interactions between the two constituents A_mB_n can be induced as a consequence of a variety of complex, interacting phenomena. The energy of the incident ions must be adjusted so that the damage energy distribution (see Fig. 2) traverses the interface. When this is the

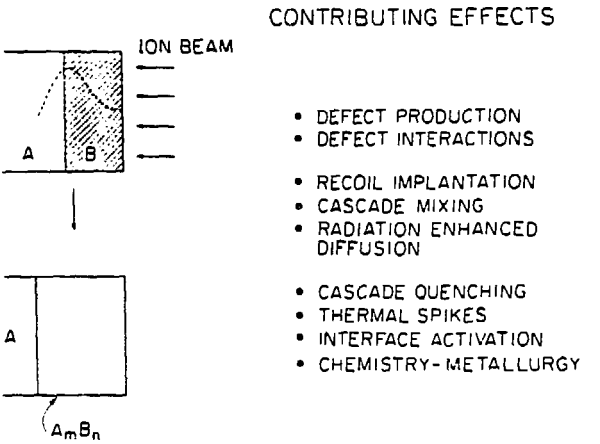

Fig. 3 - Representation of the effects contributing to ion induced materials interactions.

case the contributing effects listed in Fig. 3 can drastically alter the properties of the surface by atomic mixing and materials interactions.

Each heavy ion incident into a crystalline region of a solid initiates a collision cascade like that depicted in Fig. 4 in which huge numbers of vacancy and interstitial defects are produced by direct and secondary collisions. Some atoms of the deposited film can be recoil implanted into the substrate by direct knock-on collisions,[18] and others can be mixed by the atomic motion of the atoms within the collision cascade (cascade mixing).[19-21] These dense collision cascades can set up large concentration gradients of both vacancies and interstitials which can produce radiation enhanced diffusion,[22,23] lead to solute migration,[24] alter the near surface composition of alloys,[25,26] induce segregation or dissolution of precipitates[24] and a variety of other effects.

In addition to these ion induced processes which effectively mix the atoms in the solid, the dynamic character of each collision cascade is also important for determining the final materials interactions. The energy deposited in collision cascades such as the one shown schematically in Fig. 4 is rapidly dissipated through atomic motion in times $\sim 10^{-13}$ s. The nature of the cascade depends on the kinematics of the collision partners, but for most ion beam mixing situations (i.e., 100-500 keV heavy ions on targets of moderate to heavy masses) a large fraction of all the atoms within the cascade volume are in motion during this 10^{-13} s.[2,3,17-21] These dense cascades have been modeled by some as thermal spikes[2,18,27] in which the atoms in motion in the cascade are treated as a hot gas in equilibrium and the "heat" of the atoms in the

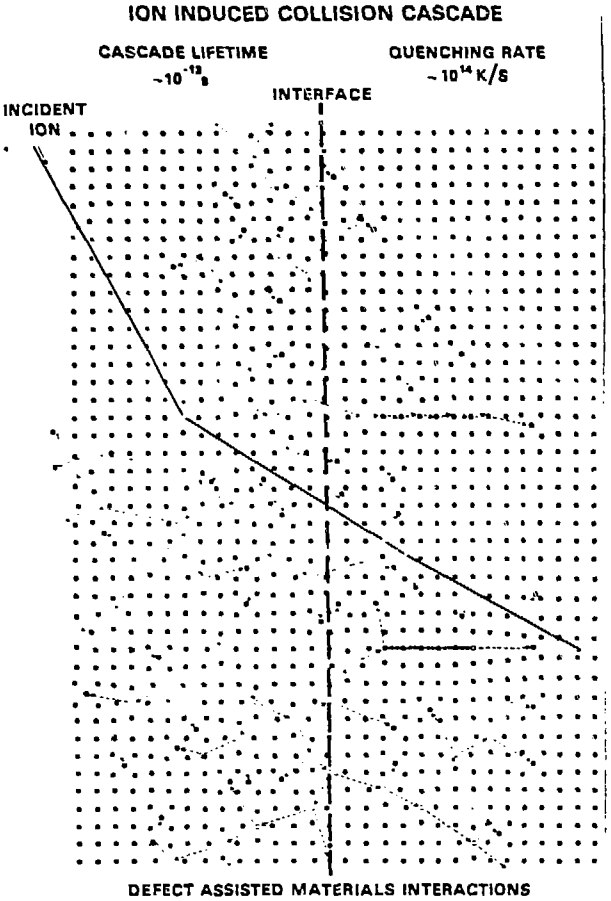

Fig. 4 - Pictorial representation of ion induced collision cascade.

cascade is conducted away from the damage region. There are several fundamental questions concerning this concept; for example, it is not clear that thermal equilibrium can be obtained on these short time scales or how the energy couples to the lattice or electronic system of the solid.[17-27] Nevertheless, whether removed by thermal conduction or atomic motion the rapid dissipation of energy from the cascade can be viewed as a rapid quenching effect with a rate ~10^{13} k/s which is comparable or greater than either vapor (~10^{10} k/s) or liquid quenching (~10^{6} k/s).[17]

The nonequilibrium nature of ion beam mixing results from the ion induced mixing, the defect production and interactions,[28] the structural modifications, and the rapid cascade quenching effects acting in concert.[17] A variety of metallurgical, chemical and thermodynamic driving forces determine the final materials alterations. In many instances the nonequilibrium nature of the interactions can alter free energy and thermodynamic constraints and make new and often unique materials interactions possible. Examples of the use of ion beam mixing to fabricate amorphous mixtures,

extended composition metglasses and equilibrium compounds will be presented later in this article.

PULSED LASER PROCESSING - Although the use of laser and electron beams for inducing materials interactions in solids is a relatively recent field of investigation it is proving an attractive alternative to conventional thermal methods.[11-17] These techniques provide precise methods to process the surface over a wide range of quenching rates. If continuous lasers are scanned or if high-power lasers with limited pulse duration (~10^{-9} to 10^{-15} s) are utilized, then only the near surface of the solid melts (heats); while in the long-time regime (> 1 ms) processing can be accomplished to greater depths. The precise control of these techniques makes it possible to accomplish surface processing of solids in either the solid or liquid phase at quenching rates projected up to as high as 10^{13} k/s.[11-17,29]

In this section we will only consider the use of pulsed lasers for studying fundamental materials interactions and initiating near surface property modifications. Pulsed annealing refers to the case in which energy is deposited into the surface region in a single pulse over areas ~1 cm in diameter. Larger areas require multiple pulses, but the annealing behavior of each pulse can be independently considered. When an energetic pulse is incident on silicon, for example, the photons are absorbed directly into the electronic system of the solid. Through electron-phonon interactions the absorbed energy is rapidly transferred to the lattice atoms as heat in times ~10^{-12} s.[29] For sufficiently intense pulses (i.e., 1-2 joules/cm^2 ruby laser pulse of 15 x 10^{-9} s duration) the near surface melts to depths ~1 μm. As the heat is conducted away to the solid substrate resolidification occurs at the liquid-solid interface, and the interface proceeds toward the sample surface at a velocity V. The melt front velocity can be controlled by the rate of energy deposition, absorption depths in the solid and liquid phases, thermal properties of the solid, etc., and can be varied from cm/s to m/s.[11-17]

The origins of new materials properties induced by pulsed laser processing are associated with this surface melting and rapid solidification. When an ion implanted solid or a composite target of two thin films are pulsed-laser annealed, the surface melts and the constituents mix by liquid diffusion. As the surface resolidifies quenching rates up to 10^{11} k/s can be readily achieved. Since this is much greater than normal splat quenching rates (~10^6 k/s) a variety of rapid solidification effects can be expected to affect the materials interactions of the mixed constituents.

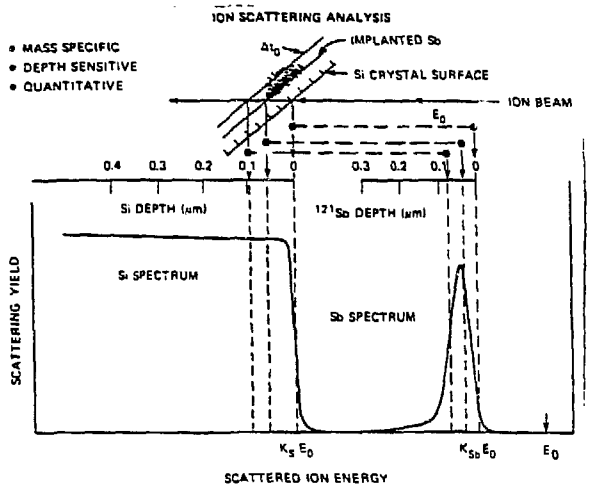

Fig. 5 - Analysis of an ion scattering spectrum for 2.5 MeV He from Sb implanted Si showing the quantitative mass and depth specificity.

ION BEAM ANALYSIS TECHNIQUES

A variety of analysis techniques are required to determine the materials properties of the ion beam and laser processed surfaces we will discuss. However, many of these are familiar techniques such as x-ray diffraction, transmission electron microscopy, electron paramagnetic resonance, etc. and need not be discussed. Ion scattering and positive ion channeling techniques are less familiar, are used often, and so will be reviewed here briefly.

ION SCATTERING - Ion scattering analysis of a silicon sample implanted with Sb ions is shown in Fig. 5. Analysis was performed by measuring the yield and energy of He^+ scattered from the implanted sample. The light He ions of incident energy E_0 undergo Rutherford elastic scattering from the atoms of the target. Their scattered energy is determined by the kinematic scattering factor K which is a function of the mass of the scattering atom. Thus, although the heavy Sb atoms are physically implanted in the near surface of the lighter host Si atoms, the energies of the He ions scattered from the two different species are separated in scattered ion energy; $K_{Si}E_0$ and $K_{Sb}E_0$ represent the energy of He^+ scattered from Si and Sb atoms respectively located at the surface. Thus ion scattering analysis is mass specific.

Since the energy loss processes for He^+ in Si are well known it is also possible to convert the scattered ion energies from Si and Sb into independent, accurate depth scales as shown at the top of Fig. 5. Finally, since Rutherford scattering is a well understood classical scattering effect, the number of He ions scattering from the target atoms at each depth can be related to the number of scattering atoms at that depth.

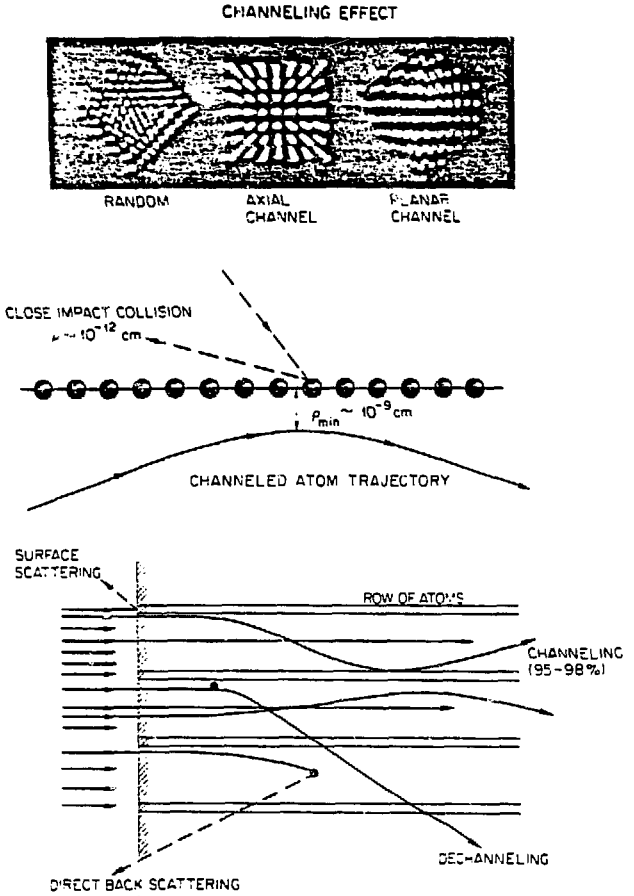

Fig. 6 - Origins of the positive ion channeling effect and its use for materials analysis.

The ion scattering analysis in Fig. 5 makes it possible to obtain a nondestructive, quantitative, depth profile of the implanted Sb. Using the known density of Si as a standard, the scattering yield from Sb at the shaded depth can be compared to the Si yield at the same depth and an accurate depth profile deduced. Depth resolutions ranging from 30 to 100 A are achievable depending on ion, target and detection conditions. For a more comprehensive discussion of ion scattering the reader is referred to a recent book.[30]

POSITIVE ION CHANNELING - A companion technique to ion scattering is the so-called channeling effect which exists for positive ions in single crystalline solids. When ions are incident along a misoriented direction of a single crystal, such as the random orientation shown in the upper left of Fig. 6, they encounter the atoms of the solid at random and have normal interaction probability and a scattering distribution like that shown in Fig. 5. However, if a well collimated beam of ions is incident along an axial or planar direction of a single crystal (see Fig. 6), then the ions no longer encounter the lattice atoms at random.

Instead the ion-atom collisions are correlated and the collective interactions of many atoms along a row or plane steers the ion away from the atoms into the open "channels" between the rows and planes of atoms (see Fig. 6). Since channeled ions never approach closer than ~10^{-9} cm to atoms on lattice sites, and since Rutherford scattering requires impact distances ~10^{-13} cm, normal scattering yields are greatly reduced for channeled ions.[30] This has several important consequences for materials analysis. Since the channeling effect exists because of crystal order it can be used as a sensor of ion induced damage. Thus it can be used to quantify in situ the damage induced by ion implantation and the annealing initiated by pulsed laser processing. Since the channeling effect alters the ion flux distribution in the channels it becomes sensitive to the location of impurity atoms in the lattice. Thus it can be used to determine lattice sites to within 0.1 A, and quantitatively measure the fraction of impurities on substitutional or interstitial sites.[30]

MATERIALS RESEARCH AND SURFACE MODIFICATIONS

Ion beam and laser processing are ideal tools for fundamental materials research because they subject materials interactions to extreme boundary conditions not normally possible. Ion bombardment and implantation offer a new dimension to materials interactions because the induced materials properties are not only determined by the characteristics of the implanted or mixed species and altered microstructures, but by cascade quenching and the complex production and interaction of defects as well. Pulsed laser processing can perform rapid heating and cooling in the solid phase; or melting, mixing and rapid solidification in the liquid phase. When coupled with conventional furnace annealing, quenching rates can be varied from 10^{4}-10^{13} k/s and resolidification melt front velocities from cm/s to m/s.

These techniques are equally useful for modifying the near-surface properties of materials to achieve beneficial properties such as reduced corrosion, improved friction and wear, etc. In this section several specific examples are presented in which the non-equilibrium aspects of ion beam and laser processing are exploited to alter surface properties. Both the fundamental materials interactions leading to property alterations, and the practical applications of these altered surfaces are discussed.

SUPERSATURATED SUBSTITUTIONAL ALLOYS OF Si - The first example to be discussed is the use of ion implantation doping and pulsed laser annealing to fabricate supersaturated substitutional alloys of silicon.[31,32] The fabrication process is depicted in Fig. 7. Implantation of any of the group III or V dopants into Si(100) results in a gaussian

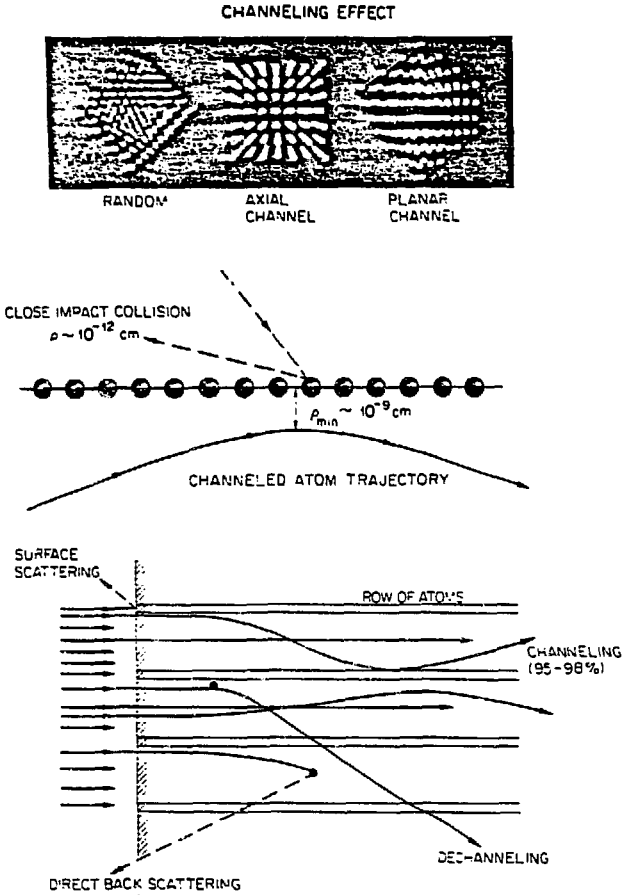

Fig. 6 - Origins of the positive ion channeling effect and its use for materials analysis.

The ion scattering analysis in Fig. 5 makes it possible to obtain a nondestructive, quantitative, depth profile of the implanted Sb. Using the known density of Si as a standard, the scattering yield from Sb at the shaded depth can be compared to the Si yield at the same depth and an accurate depth profile deduced. Depth resolutions ranging from 30 to 100 Å are achievable depending on ion, target and detection conditions. For a more comprehensive discussion of ion scattering the reader is referred to a recent book.[30]

POSITIVE ION CHANNELING - A companion technique to ion scattering is the so-called channeling effect which exists for positive ions in single crystalline solids. When ions are incident along a misoriented direction of a single crystal, such as the random orientation shown in the upper left of Fig. 6, they encounter the atoms of the solid at random and have normal interaction probability and a scattering distribution like that shown in Fig. 5. However, if a well collimated beam of ions is incident along an axial or planar direction of a single crystal (see Fig. 6), then the ions no longer encounter the lattice atoms at random.

Instead the ion-atom collisions are correlated and the collective interactions of many atoms along a row or plane steers the ion away from the atoms into the open "channels" between the rows and planes of atoms (see Fig. 6). Since channeled ions never approach closer than $\sim 10^{-9}$ cm to atoms on lattice sites, and since Rutherford scattering requires impact distances $\sim 10^{-12}$ cm, normal scattering yields are greatly reduced for channeled ions.[30] This has several important consequences for materials analysis. Since the channeling effect exists because of crystal order it can be used as a sensor of ion induced damage. Thus it can be used to quantify in situ the damage induced by ion implantation and the annealing initiated by pulsed laser processing. Since the channeling effect alters the ion flux distribution in the channels it becomes sensitive to the location of impurity atoms in the lattice. Thus it can be used to determine lattice sites to within 0.1 A, and quantitatively measure the fraction of impurities on substitutional or interstitial sites.[30]

MATERIALS RESEARCH AND SURFACE MODIFICATIONS

Ion beam and laser processing are ideal tools for fundamental materials research because they subject materials interactions to extreme boundary conditions not normally possible. Ion bombardment and implantation offer a new dimension to materials interactions because the induced materials properties are not only determined by the characteristics of the implanted or mixed species and altered microstructures, but by cascade quenching and the complex production and interaction of defects as well. Pulsed laser processing can perform rapid heating and cooling in the solid phase; or melting, mixing and rapid solidification in the liquid phase. When coupled with conventional furnace annealing, quenching rates can be varied from 10^4-10^{13} k/s and resolidification melt front velocities from cm/s to m/s.

These techniques are equally useful for modifying the near-surface properties of materials to achieve beneficial properties such as reduced corrosion, improved friction and wear, etc. In this section several specific examples are presented in which the non-equilibrium aspects of ion beam and laser processing are exploited to alter surface properties. Both the fundamental materials interactions leading to property alterations, and the practical applications of these altered surfaces are discussed.

SUPERSATURATED SUBSTITUTIONAL ALLOYS OF Si - The first example to be discussed is the use of ion implantation doping and pulsed laser annealing to fabricate supersaturated substitutional alloys of silicon.[31,32] The fabrication process is depicted in Fig. 7. Implantation of any of the group III or V dopants into Si(100) results in a gaussian

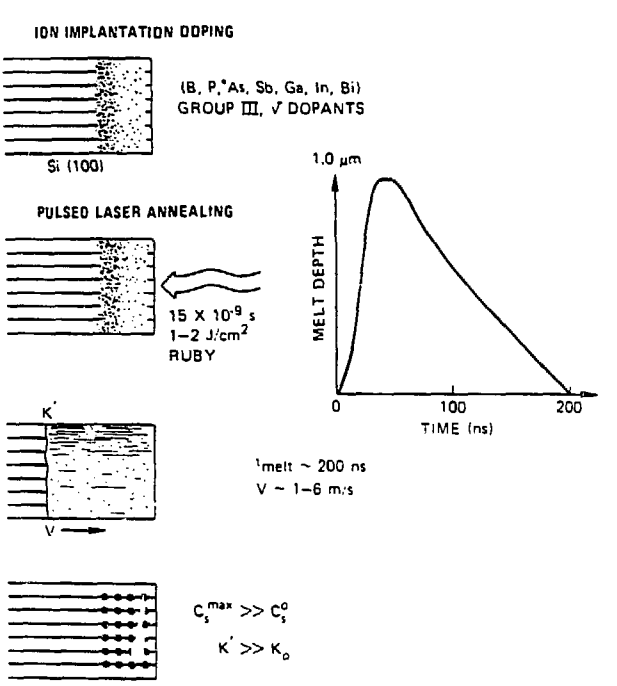

Fig. 7 - Fabrication of supersaturated substitutional alloys of Si.

profile of the dopant centered at some depth beneath the surface. As a consequence of the implantation process the Si single crystal is heavily damaged in the near-surface region and is most likely rendered amorphous. In conventional semiconductor device processing, this implanted sample would be thermally annealed to remove the damage and incorporate the dopant into an electrically active lattice sites. Since thermal annealing is an equilibrium processing method the maximum dopant concentration which could be incorporated into substitutional sites would be limited by the equilibrium solid solubility limit C_s^o.

An alternative to this annealing process is to utilize a single pulse from a Q-switched ruby laser (1-2 joules/cm^2, 15 x 10^{-9} s duration) to anneal the implanted sample. When this is done the sample melts to a depth well beyond the depth of the implanted dopant. While the surface is molten the dopant mixes by liquid diffusion. As the heat is conducted away to the underlying substrate the near surface solidifies.

For the present conditions the position of the melt front versus time behaves as shown by the insert in Fig. 7. The surface of the Si melts to a depth of ~1 μm very rapidly and, as conductive cooling occurs, the meltfront proceeds back toward the surface at a velocity of several meters/second, depending on the exact annealing conditions. This entire process

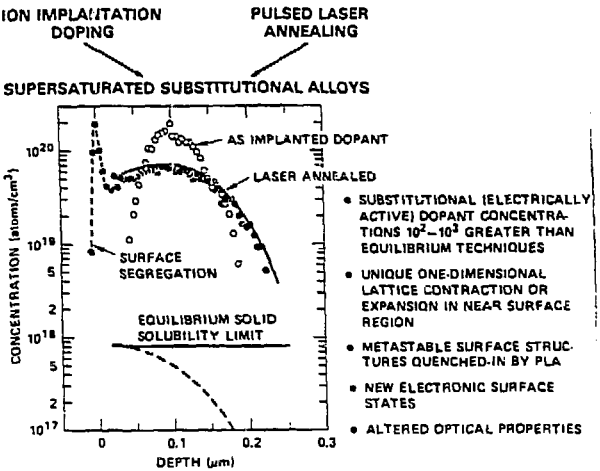

Fig. 8 - Concentration vs. depth profiles for Bi implanted Si and the associated materials alterations.

is over in a few hundred nanoseconds. As a consequence of this extremely rapid solidification several phenomena occur which are unique to this fabrication method. First, even at these extreme velocities, perfect, liquid-phase, epitaxial crystallization of the molten silicon occurs on the underlying single crystal substrate. Second, as this crystallization occurs the distribution coefficient at the liquid/solid interface, K', mediates the concentration of dopant that can be incorporated into substitutional sites in the solid. Because of the nonequilibrium nature of this crystallization process K' is much greater than the equilibrium distribution coefficient K_o, and dopant atoms are incorporated into substitutional sites by solute trapping at concentrations C_s^{max} much greater than the maximum allowed equilibrium concentrations C_s.[31,32] Thus the term supersaturated substitutional alloys.

Some of the new materials properties of these alloys are highlighted in Fig. 8. The inserted figure shows the concentration versus depth profiles extracted from ion scattering analyses of Bi implanted Si(100) before and after laser annealing.[32] The open circles show the as-implanted dopant distribution centered at the implanted depth of about 0.1 μm. As a consequence of pulsed laser annealing the near surface melts to ~0.6 μm, the Bi diffuses in the molten Si, and as the sample crystallizes Bi is trapped into the solid with the profile shown by the solid circles in Fig. 8.

Ion channeling measurements made to determine the fraction of Bi on substitutional lattice sites after laser annealing showed that ~98% was substitutional up to a depth <0.02 μm where some surface segregation of

Table I - Fundamental Mechanisms Limiting Substitutional Solubilities in Si V = 4.5 m/s

1. THERMODYNAMIC LIMIT

DOPANT	C_S^0 (cm^{-3}) EQUILIBRIUM	C_S^{max} (cm^{-3}) (100)	C_S^{max} (cm^{-3}) (111)	FUNCTIONAL DEPENDENCE
IV / As	1.5×10^{21}	6.0×10^{21}	6.0×10^{21}	$C_S^{max} = C_S^{max}$ (V, hkl)

2. MECHANICAL STRAIN

DOPANT	C_S^0 (cm^{-3}) EQUILIBRIUM	C_S^{max} (cm^{-3}) (100)	C_S^{max} (cm^{-3}) (111)	FUNCTIONAL DEPENDENCE
III / B	6.0×10^{20}	2.0×10^{21}	2.0×10^{21}	UNIQUE LATTICE ALTERATION

3. INTERFACIAL INSTABILITIES AND/OR
4. PRECIPITATE FORMATION (PHASE SEPARATION)

DOPANT	C_S^0 (cm^{-3}) EQUILIBRIUM	C_S^{max} (cm^{-3}) (100)	C_S^{max} (cm^{-3}) (111)	FUNCTIONAL DEPENDENCE
V / Sb	7.0×10^{19}	2.0×10^{21}	2.0×10^{21}	(3)
Bi	8.0×10^{17}	4.0×10^{20}	8.6×10^{20}	(3, 4) $K^{\perp}(111) > K^{\perp}(100)$, $C_S^{max} = C_S^{max}$ (V, hkl), II – HIGH V, PF – LOW V
IV / Ge	5.0×10^{20}	6.0×10^{21}	$> 1.2 \times 10^{22}$	(3)
Sn	5.5×10^{19}	9.6×10^{20}	1.4×10^{21}	(3)
Pb	---	1.0×10^{20}	3.0×10^{20}	(3, 4)
III / Ga	4.5×10^{19}	4.5×10^{20}	7.2×10^{20}	(3)
In	8.0×10^{17}	1.5×10^{20}	4.5×10^{20}	(3, 4)
Tl	---	---	---	(4) COHERENT PRECIPITATES

excess Bi had occurred (dashed lines).[30] The maximum equilibrium solid solubility for Bi in Si is marked on Fig. 8, and for these particular annealing conditions the total substitutional concentration of Bi exceeds this equilibrium limit by a factor of ~500.

There are numerous opportunities for fundamental materials research afforded by the fabrication of these supersaturated alloys and the investigation of their materials properties after fabrication. One such continuing study has been to determine the fundamental mechanisms which limit the maximum substitutional concentrations for the various dopants.[31,32] It was found that the group III-V dopants in Si were limited by one of four mechanisms and results from this study are summarized in Table I. Ion scattering/channeling analysis was used to measure the maximum concentrations of the various dopants that could be incorporated into both (100) and (111) oriented samples by ion implantation doping and pulsed laser annealing. The annealing conditions were such as to give a melt front velocity during solidification of 4.5 m/s. Ion channeling measurements of maximum concentrations were coupled with x-ray scattering, transmission electron microscopy, electrical measurements, etc. as required to identify the limiting mechanisms.

The absolute maximum solid solubility limits for each dopant can be predicted from

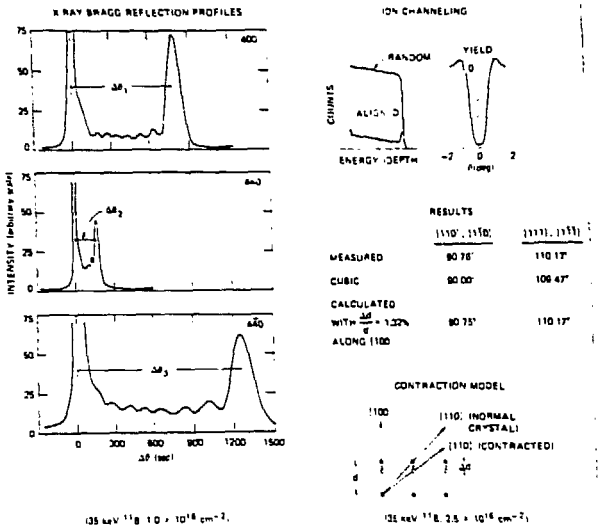

Fig. 9 - Ion channeling and x-ray diffraction analysis of the one dimensional lattice contraction of B implanted and laser annealed Si.

thermodynamic calculations.[33] As indicated in Table I only As achieves this thermodynamic limit by V = 4.5 m/s. Experiments at higher velocities show the same measured maximum. The dopant B is limited by mechanical strain before reaching the thermodynamic limit and the origins of this will be discussed later in this section in connection with the unique lattice alteration which causes this. The remainder of the dopants are limited either by interfacial instabilities or precipitate formation or both as indicated in Table I.

The unique lattice alterations which occur in these supersaturated substitutional alloys, and which limit the maximum B concentration due to mechanical strain as indicated in Table I, have been studied by a combination of x-ray diffraction and ion channeling techniques.[34,35] A composite of results are shown in Fig. 9. Both the x-ray Bragg reflection profiles and ion channeling results from a Si(100) sample implanted with 1 x 10^{16} B/cm^2 at 35 keV, and laser annealed show that the B supersaturated alloy has undergone a unique lattice alteration as shown schematically in the lower right hand corner of Fig. 9.[34,35] As the ion-implanted, laser-annealed sample recrystallizes by liquid-phase epitaxy, the B is incorporated into substitutional sites in a perfect Si lattice at supersaturated concentrations. Since the size of B is smaller than Si the lattice contracts on crystallization in the heavily doped surface region. However, because of the absence of any extended dislocations, the surface undergoes a one dimensional contraction normal to the surface as illustrated.[34,35] The result is a heavily doped surface layer with a noncubic lattice contraction of ~1.3% normal to the surface of the crystal. This surface is under considerable strain and as larger and larger concentrations of B are incorporated into

substitutional sites the strain increases until the surface mechanical strain exceeds the fracture strength of Si and the surface layer cracks. This mechanical strain limits the maximum B concentration.

As indicated by the highlights in Fig. 8 the processing of these supersaturated substitutional alloys also leads to some new and unusual surface properties as well as the unique lattice alterations just discussed. For example, the extremely rapid melting and liquid phase epitaxial recrystallization can result in a quenched-in metastable surface structure.[37-39] When the Si(111) surface is sputter-cleaned and thermally annealed in ultrahigh vacuum (equilibrium processing) the atomically clean surface atoms reorder to form the complex (7x7) structure. However, if the same surface is processed with a single laser pulse (nonequilibrium processing) the surface melts and resolidifies so rapidly that an atomically clean surface with a simple (1x1) low energy electron diffraction pattern characteristic of the bulk atomic arrangement is produced.[37] If this same pulsed-laser processing is applied to ion implanted (doped) Si surfaces, supersaturated alloys are produced with surface electronic properties very different than conventionally doped Si.[37-39]

The flexibility of pulsed laser processing can be used to increase quenching rates, or meltfront velocities, over a wide range. In Si, for example, UV lasers have been used to study crystallization phenomena as a function of melt front velocity, and above about 15 m/s the solidification becomes so rapid that crystallization is not possible and the amorphous state is quenched at the surface.[40,41] Combining continuous, scanned, and pulsed laser and electron beam processing with conventional furnace annealing it is now possible to study crystallization; the kinetics of interfaces, precipitation and segregation; interfacial instabilities; undercooling or superheating; and a host of other phenomena at solidification velocities from $\sim 10^{-10}$ to $\sim 10^{2}$ m/s.[11-17,31,41]

CERAMIC AND INSULATOR PROCESSING - Ceramic and insulating materials are particularly amenable to surface modifications because they bridge such a broad spectrum of materials properties. Bonding can vary from ionic to covalent to near metallic, so injected dopant atoms can induce a variety of changes; since damage can occur by both ionizing as well as displacement collisions, induced microstructural changes can vary widely. Ion beam modifications have included optical properties,[8,42-44] phase structure alterations,[8,42-44] electrical and/or chemical properties,[8,42-44] and mechanical properties.[45-49] Ion beam mixing has been used to increase adherence of metal films to insulators[44,49] and to alter the structural and conducting properties of polymers.[50]

The potential for alteration of the surface mechanical properties of Al_2O_3 by ion

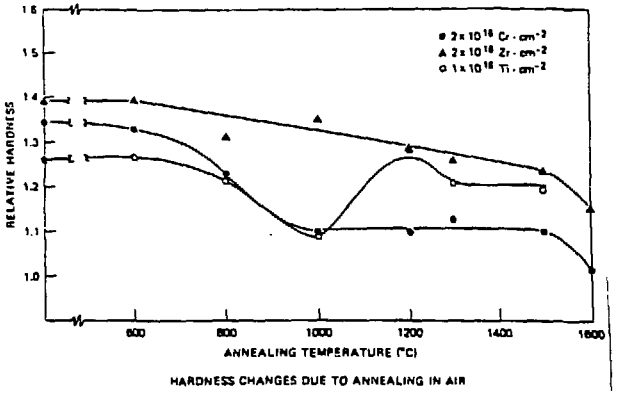

Fig. 10 - Measurements of the hardness of implanted Al_2O_3 relative to unimplanted as a function of annealing in air.

implantation doping can be seen from the results in Fig. 10 which show the relative hardness increases that can be achieved by implantation of Cr, Zr, and Ti and the effects of annealing in air.[46,48,49] Not only can the surface hardness be increased by implantation, as shown in Fig. 10, but the fracture toughness can be increased ~20%. These investigations showed that the improved mechanical properties depended sensitively on the doping species and implantation conditions.[46-49] Implantation of Cr suffered a loss of hardness at temperatures ~900°C because it became incorporated into Al lattice sites on annealing to form Al_2O_3-Cr_2O_3 solid solutions; while Zr, which is insoluble in Al_2O_3, retained its hardness to temperatures near 1600°C. When SiC[47] was implanted at room temperature or Al_2O_3 at liquid nitrogen temperature[51] the surfaces became amorphous and surface hardness decreased while fracture toughness increased. These combined results show that surface mechanical properties can often be tailored to achieve the desired properties.

The pronounced differences in relative hardness versus annealing temperature shown in Fig. 10 for the various dopants are mirrored by changes in the structural properties at the surface. By utilizing ion channeling measurements like those shown in Fig. 11 it is possible to monitor the ion induced lattice damage and its recovery on annealing, the diffusion behavior of the implanted Cr, and even the specific sublattice sites acquired by Cr on annealing.[46,48,49] Because of the kinematic separation of ions scattered from the Al and O sublattices and the implanted Cr in Fig. 11, it is possible to monitor the damage recovery as a function of annealing temperature. The ion channeling effect can be utilized to deduce that Cr goes substitutionally into the Al sublattice at temperatures ~1200°C and EPR shows that the Cr is accommodated as Cr^{3+}.[46,48,49]

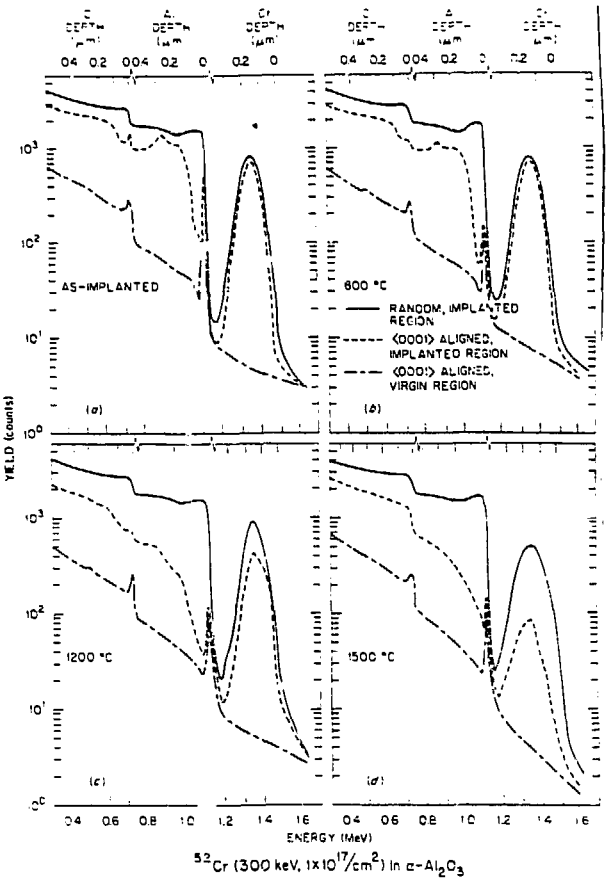

Fig. 11 - Ion channeling of the damage and annealing behavior of Cr implanted Al_2O_3.

Ion beam and laser mixing of metal films on Al_2O_3, SiC and Si_3N_4 has also proved quite successful for increasing the mechanical properties of the surface and the adhesion of the metal films.[49,52,53]

ION BEAM AND LASER PROCESSING OF SUPERCONDUCTING MATERIALS - Ion beam and laser processing techniques are well suited to the fabrication and study of superconducting materials for several reasons. First, materials alterations usually result in a change in the superconducting transition temperature T_c and this can be easily monitored in situ during both ion beam and laser processing. Second, only a surface layer the order of the coherence length for superconductivity (<0.05 μm) need be altered in order to induce a measurable change and this is much less than the normal near surface modification depths using the ion beam and laser techniques. Third, many high T_c materials are the result of some metastable processing and since ion beam and laser processing are both non-equilibrium methods they should be particularly applicable. Several specific examples exploiting these advantages are given below and recent reviews cover the earlier work in this field.[54-56]

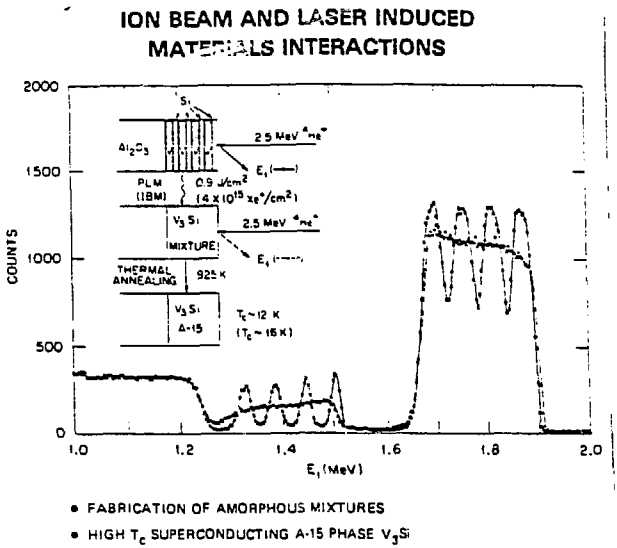

Fig. 12 - Fabrication of superconducting V_3Si by ion beam and pulsed laser mixing.

The use of ion beam and pulsed laser mixing to fabricate superconducting V_3Si from V and Si thin films is represented by the results in Fig. 12.[17,57-59] The ion scattering analysis in Fig. 12 shows that the multilayer V/Si samples used were designed to limit the composition near V_3Si and consisted of four V layers separated by four Si layers prior to mixing. Mixing was induced by either bombardment with 4×10^{15} Xe^+/cm^2 or a single 15 ns pulse from a ruby laser at 0.9 J/cm^2. In both instances the ion scattering shows complete mixing and this was confirmed by cross-section TEM analysis. The mixture was amorphous with a composition $V_{2.8}Si$ and was not superconducting. Thermal annealing to only 500°C resulted in the nucleation of the superconducting A-15 phase from this amorphous mixture.[57] In the case of ion beam mixing the superconducting character of the film was as good as high-temperature thermally processed V_3Si with $T_c \sim 16$ K.[59] The pulsed laser mixed films on the other hand had $T_c \sim 10$-12 K and, even when the laser mixed samples were thermally annealed to temperatures as high as 925 K, their T_c's were always less than multilayer samples (not laser annealed) thermally prepared at the same temperature.[57,58] This is related to laser induced defects which are much more difficult to anneal than ion induced damage. These results and the effects associated with multiple laser pulses, pulse length, and the whole question of defects in A-15 superconductors, etc. are discussed elsewhere.[17,57]

In general both theory and experiment show that T_c can be increased by increasing the density of states near the Fermi surface or with enhanced phonon softening.[54-56] Quite often electronic or compositional changes can

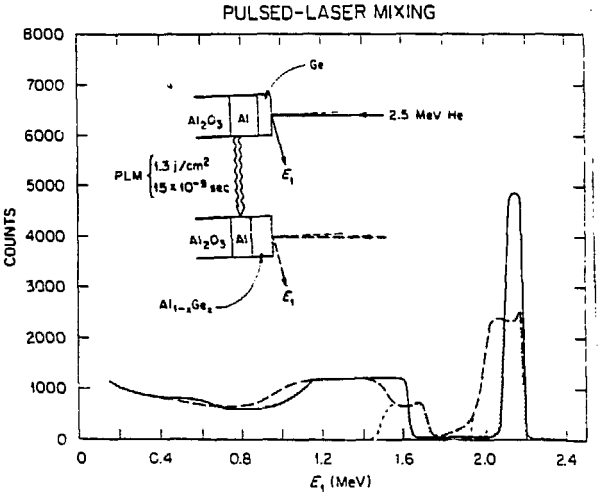

Fig. 13 - Ion scattering analysis of amorphous metglass mixtures of Al/Ge fabricated by pulsed laser mixing.

be induced by implanting the proper impurities, and ion damage can alter the phonon spectrum.[17,54-56] An example of the latter is recent low temperature He^+ irradiation experiments on Pd metal.[59] This metal has a high density of states near the Fermi level and a phonon spectrum favorable for superconductivity but shows no superconductivity as low as 1.7 mK. However, irradiation with He^+ at low temperature transforms Pd into a superconductor with $T_c \sim 3$ K.[60]

An interesting example of beneficial laser processing concerns pulsed laser heating of Nb_3Ge.[57,61] Pulsed laser melting of the metastable high T_c ($T_c \sim 22$ K) phase of Nb_3Ge initiates the formation of the stable Nb_5Ge_3 phase and a decrease in T_c. However, controlled rapid heating of Ge-rich Nb_3Ge can be used to produce finely dispersed stable phase precipitates which act as flux pinning sites and increase the critical current density J_c without decreasing T_c.[61]

AMORPHOUS METAGLASSES AND METASTABLE PHASE FORMATION - Normally metal/semiconductor systems can be quenched from the melt to form amorphous metglasses only at compositions near the eutectic compositions when conventional methods such as splat quenching are used. However, since pulsed laser quenching can be 10^2-10^3 times greater it is possible to form amorphous metglasses over a greatly extended range of compositions.[17,57,58,62,63]

An example of pulsed laser mixing of the eutectic Al/Ge system is depicted in Fig. 13. A thin film of Ge was vapor deposited on a thin film of Al on an Al_2O_3 substrate as shown by the ion sattering analysis (solid lines) in Fig. 13. A single laser pulse from a Q-switched ruby laser (1.3 J/cm^2, 15 x 10^{-9} s) was used to melt the near surface as illustrated. The absorbed energy melted part

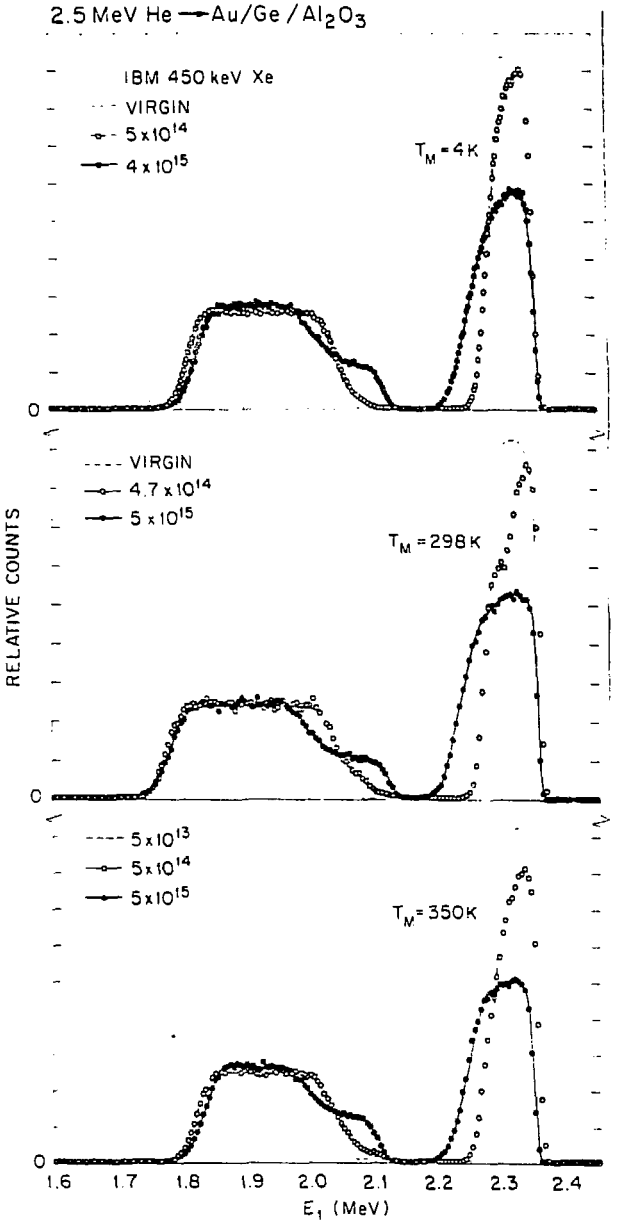

Fig. 14 - Ion scattering analysis of the Au/Ge metglass $Au_{50}Ge_{50}$ fabricated by ion beam mixing.

way through the Al film, the Al and Ge mixed by liquid diffusion, and as the molten surface cooled an amorphous mixture was formed at a composition determined by the relative amounts of Ge and Al present in the molten surface layer (dash line, Fig. 13). It is possible to control the compositions of Al and Ge by making limited supply thin film composite samples like the V and Si films of Fig. 12. If this is done virtually any composition of Al and Ge can be quenched into an amorphous metglass.

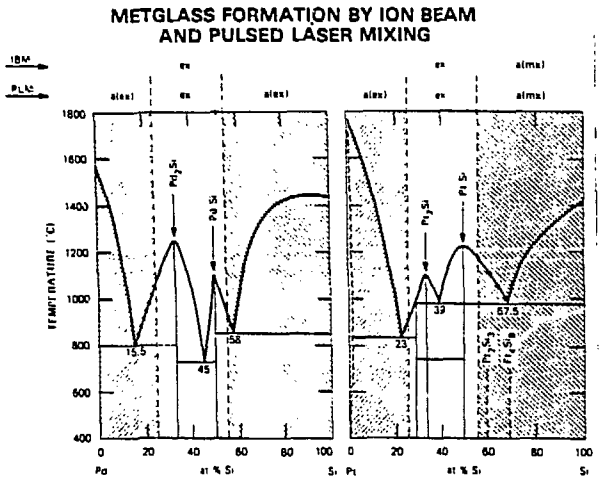

Fig. 15 - Summary of ion beam and laser processing results for Pd/Si and Pt/Si (see text).

Ion beam mixing can also be used to form amorphous mixtures as depicted by the results in Fig. 14 for the Au/Ge eutectic system.[17] In this case Au on Ge on Al_2O_3 was bombarded with increasing doses of 450 keV Xe ions with the samples held at temperatures of 4, 298, and 350 K. Analysis of these ion scattering spectra[17] shows that by about 5 x 10^{15} Xe/cm^2 the Au films are consumed and mix with the Ge to form an amorphous mixture. There are however some anomalous features in this instance. First, the plateau in the scattering from the Ge film after mixing (filled circles) shows that the Au and Ge mixed at a definite composition, $Au_{50}Ge_{50}$. If thicker Au films are used, thicker amorphous mixtures are formed at the surface, but always at the same composition $Au_{50}Ge_{50}$.[17,62] Second, if this amorphous mixture is allowed to anneal at room temperature or heated <100°C a metastable crystalline phase forms from the amorphous mixture at the $Au_{50}Ge_{50}$ composition.[17,62] This general trend has been found in the Au/Si system as well where an amorphous mixture and a new metastable crystalline phase forms at the composition Au_5Si_2.[17,62,64] In both these cases, the same metastable phases can be produced from amorphous mixtures made by pulsed laser mixing[17,62] and they have not been reported from conventional splat quenching studies.

Ion beam and pulsed laser mixing can also form extended composition metglass mixtures (and metastable phases) in silicide forming systems as the schematic representation in Fig. 15 indicates. This figure attempts to abstract the results of several researchers and the reader is referred to references 17, 58, 59, 64, and 65 for an accurate account of the work. By using thin film composite targets of Pt/Si or Pd/Si to control the compositions of the mixtures, these researchers found that amorphous metglass mixtures could

be made over the entire shaded ranges by either ion beam or pulsed laser mixing. Furthermore, when the Si rich amorphous mixtures of Pt/Si were thermally annealed two new metastable phases, Pt_2Si_3 and Pt_4Si_9 were formed as shown by the dotted lines on the figure.

SUMMARY

The examples presented here merely suggest the potential of ion beam and laser processing for both fundamental materials studies and practical applications. Many of the fundamental ion beam mixing mechanisms leading to new materials properties are not well understood and need more detailed study.[17] For example it is not clear why Au/Ge and Au/Si form amorphous mixtures at the same compositions as the metastable phases which result on thermal annealing; or why, despite the similarity of phase diagrams for Pd/Si and Pt/Si, that Pt/Si forms metastable phases while Pd/Si does not. Although the Au/Ge eutectic systems undergo prolific ion beam mixing at all temperatures, Al/Ge, which is also a eutectic system, does not mix at all.[17]

For practical applications ion beam and laser processing are appropriate for virtually any material and for alteration of any surface related phenomenon. The added dimension of these processing methods are their nonequilibrium capabilities which can lead to new surface alterations. Their primary limitation is the near-surface (<10 μm) modification depths.

REFERENCES

1. Proceedings of the Third International Conference on Ion Beam Modification of Materials, Nucl. Inst. Meth. 209/210, 1983.
2. Ion Implantation and Beam Processing, ed. by J. M. Poate and J. S. Williams, Academic Press, 1984.
3. Metastable Materials Formation by Ion Implantation, ed. by S. T. Picraux and W. J. Choyke, North Holland, New York, 1982.
4. G. Dearnaley, J. H. Freeman, R. S. Nelson and J. Stephen in Ion Implantation, North Holland, Amsterdam, 1973.
5. P. D. Townsend, J. C. Kelly and N.E.W. Hartley in Ion Implantation, Sputtering and Their Applications, Academic Press, London, 1976.
6. J. W. Mayer, Lennart Eriksson and J. A. Davies in Ion Implantation in Semiconductors, Academic Press, New York, 1970.
7. Ion Implantation and Ion Beam Processing of Materials, ed. by G. K. Hubler, O. W. Holland, C. R. Clayton, and C. W. White, North Holland, New York, in press.
8. Proceedings of the Ion Beam Modification of Materials Conference, SUNY Albany, Albany, New York, July 14, 1980, Nucl. Instr. Meth. 182/183, (1981).

9. Ion Implantation Metallurgy, ed. by C. M. Preece and J. K. Hiroven, The Metallurgical Society of AIME Conference Proceedings, 1980.
10. Ion Implantation Treatise on Materials Science and Technology, Vol. 18, ed. by J. K. Hirvonen, 1980.
11. Laser-Solid Interactions and Transient Thermal Processing of Materials, ed. by J. Narayan, W. L. Brown, and R. A. Lemons, North Holland, 1983.
12. Laser Annealing of Semiconductors, ed. by J. M. Poate and J. W. Mayer, Academic Press, 1982.
13. Laser and Electron-Beam Interactions with Solids, ed. by B. R. Appleton and G. K. Celler, North Holland, New York, 1982.
14. Laser-Solid Interactions and Laser Processing-1978, ed. by S. D. Ferris, H. J. Leamy and J. M. Poate, American Institute of Physics No. 50, 1979.
15. Laser and Electron Beam Processing of Materials, ed. by C. W. White and P. S. Peercy, Academic Press, New York, 1980.
16. Laser and Electron Beam Solid Interactions and Materials Processing, ed. by J. F. Gibbons, L. D. Hess, and T. W. Sigmon, North Holland, New York, 1981.
17. B. R. Appleton, Chapter 7 in Ref. 2.
18. R. S. Nelson, Rad. Eff. 2, 47 (1969).
19. H. H. Andersen, Appl. Phys. 18, 131 (1979).
20. P. Sigmund and A. Gras-Marti, Nucl. Inst. Meth. 182/183, 25 (1981).
21. U. Littmark and W. O. Hofer, Nucl. Inst. Meth. 168, 329 (1980).
22. R. Sizmann, J. Nucl. Mater. 69/70, 386 (1978).
23. S. M. Myers, Nucl. Inst. Meth. 168, 265 (1980).
24. A. D. Marwick and R. C. Piller, Nucl. Inst. Meth. 182/183, 121 (1981) and references therein.
25. L. E. Rehn, p. 17 in Ref. 3.
26. P. R. Okamoto et al., J. Nucl. Mater. 108/109, 319 (1982).
27. J. A. Davies, Chapter 4 in ref. 2.
28. N. L. Peterson and S. D. Harkness, eds., Radiation Damage in Metals. American Society for Metals, Metals Park, Ohio, 1975.
29. N. Bloembergen, H. Kurz, J. M. Liu, and R. Liu, p. 1 in Ref. 13.
30. Backscattering Spectrometry, ed. by W. K. Chu, J. W. Mayer, and M. A. Nicolet, Academic Press, New York, 1978.
31. C. W. White, B. R. Appleton, and S. R. Wilson, Chapter 5 in Ref. 12.
32. C. W. White, S. R. Wilson, B. R. Appleton and F. W. Young, Jr., J. Appl. Phys. 51, 738 (1980).
33. J. W. Cahn, S. R. Coriell, and W. J. Boettinger, p. 89 in Ref. 15.
34. B. C. Larson, C. W. White and B. R. Appleton, Appl. Phys. Lett. 32, 801 (1978).

35. B. R. Appleton et al., p. 291 in Ref. 14.
36. J. Narayan and O. W. Holland, Appl. Phys. Lett. 41, 239 (1982); and J. Narayan, O. W. Holland and B. R. Appleton, J. Appl. Phys., in press.
37. C. W. White, D. M. Zehner, S. U. Campisano and A. G. Cullis, Chapter 4 in Surface Modification and Alloying, ed. by J. M. Poate, G. Foti, and D. C. Jacobson, Plenum Press, p. 81, 1983, and references therein.
38. D. E. Eastman et al., Phys. Rev. B 24, 3647 (1981).
39. D. M. Zehner et al., Appl. Phys. Lett. 37, 456 (1980).
40. G. J. Galvin, M. O. Thompson, J. W. Mayer, P. S. Peercy, R. B. Hammond and N. Paulter, Phys. Rev. B 27, 1079 (1983).
41. Michael O. Thompson, J. W. Mayer, A. G. Cullis, H. C. Weber, N. G. Chew, J. M. Poate and D. C. Jacobson, Phys. Rev. Lett. 50, 896 (1983).
42. Proceedings of the Third International Conference on Ion Beam Modification of Materials, Nucl. Inst. Meth. 209/210, 1983.
43. P. D. Townsend, J. C. Kelly and N.E.W. Hartley in Ion Implantation, Sputtering and Their Applications, Academic Press, London, 1976.
44. Proceedings of Radiation Effects in Insulators, May 30-June 3, 1983, Albuquerque, NM, Nucl. Inst. Meth.in Physics Research B1, 1984.
45. Metastable Materials Formation by Ion Implantation, ed. by S. T. Picraux and W. J. Choyke, North Holland, New York, 1982.
46. C. J. McHargue, H. Naramoto, B. R. Appleton, C. W. White, and J. M. Williams, ibid 3, p. 147.
47. J. M. Williams, C. J. McHargue, and B. R. Appleton, Proc. of the Ion Beam Modification of Materials Conf., Sept. 6-10, 1982, Grenoble, France, Nucl. Instr. and Meth. 209/210, 1983.
48. H. Naramoto, C. W. White, J. M. Williams, C. J. McHargue, O. W. Holland, M. M. Abraham, and B. R. Appleton, J. Appl. Phys. 54, 683 (1983).
49. B. R. Appleton et al., in Ref. 44, p. 167.
50. B. S. Elman et al., Phys. Rev. B 25, 4142 (1982), and Phys. Rev. B 24, 1027 (1981).
51. C. W. White et al., in Defect Properties and Processing of High-Technology Non-metallic Materials, ed. by J. H. Crawford, Jr., Y. Chen, and W. A. Sibley, North Holland, New York, in press.
52. J. Narayan et al., J. Appl. Phys., in press.
53. C. W. White et al., Materials Letters, in press.
54. B. Stritzker, J. Nucl. Mater. 72, 256 (1978).
55. O. Meyer, Rad. Eff. 48, 51 (1980).
56. H. Bernas and P. Nedellec, Nucl. Inst. Meth. 183, 845 (1981).

57. B. R. Appleton et al. in Ref. 16, p. 607.
58. B. Stritzker, B. R. Appleton, C. W. White, S. S. Lau, Solid State Commun. 41, 321 (1982).
59. S. S. Lau, J. W. Mayer, B. Y. Tsaur, and M. von Allmen in Ref. 15, p. 511.
60. J. D. Meyer and B. Stritzker, Phys. Rev. Lett. 48, 502 (1982).
61. A. I. Braginski et al., Appl. Phys. Lett. 39, 277 (1981).
62. S. S. Lau, B. Y. Tsaur, M. von Allmen, J. W. Mayer, B. Stritzker, C. W. White and B. R. Appleton, Nucl. Inst. Methods 182/183, 97 (1981).
63. M. von Allmen et al. in Ref. 16, p. 559.
64. J. W. Mayer, B. Y. Tsaur, S. S. Lau, and L. S. Hung, Nucl. Inst. Meth. 182/183, 1 (1981).
65. M. von Allmen et al. in Ref. 16, p. 559.